Letters on materials 7 (4), 2017 pp. 459-464 www.lettersonmaterials.com

DOI: 10.22226/2410-3535-2017-4-459-464 PACS 81.20.–n, 81.40.Gh, 81.40.Lm, 81.70.–q

Effect of the initial state on nanostructuring and strengthening of middle- and high-strength age-hardenable aluminum alloys under severe plastic deformation (Review)

M. V. Markushev†, E. V. Avtokratova, O. Sh. Sitdikov

†mvmark@imsp.ru

Institute for Metals Superplasticity Problems of RAS, Khalturin St., 39, Ufa, 450001, Russia

General requirements to the initial structure and phase composition of commercial middle- and high-strength age-hardenable aluminum alloys, especially to the parameters of precipitates of main strengthening phases and transition metals aluminides, which are important for nanostructuring of the alloys matrix under processing, involving severe plastic deformation (SPD), preliminary and post-SPD heat treatment, are reviewed. The data on the structure, hardness and tensile strength found in disc-shape samples severely deformed via room temperature high pressure torsion (HPT) are analyzed. The role of precipitates in grain refinement down to nanoscale sizes is demonstrated. Influence of the origin, morphology and densities of precipitates on the efficiency of nanostructuring and strengthening of the alloys is analyzed. Structure-strength relations, evolution of grain and second phase structure parameters prior to, during, and after SPD are discussed. It is concluded that in order to obtain high-strength nanostructured states, the alloys should be deformed in a preliminarily quenched state. Post-SPD aging of preliminarily quenched and underaged alloys can provide them extra hardening up to 15%. A contribution of the SPD-induced formation of nanosized subgrain/grain boundary networks on the strength of alloys does not exceed that of dispersion hardening by conventional aging.

Keywords: aluminum alloy, severe plastic deformation, precipitates, nanostructuring, recrystallization.

1. Introduction

In recent decades, thermomechanical treatment aimed at nanostructuring (nanoTMT) of widely used commercial middle- and high-strength age-hardenable Al alloys has been actively developed. Nanostructuring commonly means the reduction in size of phase components of alloys or even one of their structural parameter down to hundred nanometers or less [1 – 3]. One of the potentially industrial methods of nanostructuring was realized in a number of techniques collected under a term of so-called severe plastic deformation (SPD) [4 – 10]. The nature and technical aspects of SPD have been described in a plenty of studies. However, many points do not still have a systematic description and remain undisclosed. Among them is the effect of initial material state on the structure and related properties developed. So, general requirements for efficient nanostructuring and, most importantly, on structural principles of its control are still absent.

Since the Al alloys are mostly complex systems containing a number of primary and secondary phases, understanding their role in nanoTMT is strongly required. Especially, the role of precipitates in developing the structure of the alloy matrix should be considered. By the origin and morphology these phases are commonly divided into two groups. The first one belongs to so-called dispersoids with a diameter up to hundreds of nanometers. They are formed during hot processing of an ingot due to decomposition of the aluminum solid solution supersaturated by transition metals (TM). The second one includes zones and precipitates of main strengthening phases forming under natural and/or artificial aging of pre-quenched (Q) cast or wrought products. Their sizes can reach several microns after long-term heterogenization annealing at temperatures below solvus point [11 – 14]. Under conventional TMT these precipitates stimulate nucleation of centers of discontinuous recrystallization (particle stimulated nucleation effect) [14 – 16], while dispersoids suppress dislocation rearrangement (dynamic recovery) and grain growth owing to Zener effect [7, 16, 17], stabilizing their size. The significance of both effects for nanostructuring seems to be important, since SPD is more frequently accompanied by fragmentation and continuous dynamic recrystallization and post-SPD annealing results in poligonization and discontinuous/continuous static recrystallization [6, 7, 9, 17]. According to [16, 18], formation and transformation of low-angle boundaries into high-angle ones (LABs into HABs) occur more intensely, when the LABs are stabilized by disperse phases. However, in their presence more diffuse intergranular boundaries can be formed and this, on the contrary, hinders their conversion into HABs [16, 19].

The high potential of nanoTMT for conventional cast and wrought Al alloys has been shown in numerous studies. It is also announced as quite an efficient commercial route to enhance their service and functional properties [20 – 27]. In this regard, optimization of the matrix structure of alloys and its heterogeneity (sizes, distributions and densities of second

phases) before SPD comes to the forefront, because properties of the final product are conditioned by initial structure/phase state and its subsequent transformations under processing.

Thus, the purpose of the paper is to review some recent data obtained by the authors and to elucidate the potential of the effect of initial alloy condition, in particular the size of grains and secondary phases, on the structure and strength of SPD-processed commercial middle- and high-strength age-hardenable Al alloys. For that, evolution of their structure/property relations under SPD, preliminary and post-SPD heat treatment will be considered for the most powerful nanostructuring technique, high pressure torsion (HPT) [4, 7, 10, 27].

2. Results and discussions

2.1. Effect of prior SPD aging

The complex effect of severe straining and nanosized precipitates of both TM aluminides and main strengthening phases was analyzed for Zr modified 7475 high-strength (Al-6.0Zn-2.5Mg-1.8Cu-0.23Cr-0.16Zr) alloy [28]. The chill cast ingot was preliminarily homogenized at 490°C for 20 hrs and water quenched from 475°C to provide matrix supersaturated by Zn, Mg and Cu and homogeneously distributed dispersoids. Part of samples was further under-aged (UA) at 120°C for 8 hrs to add nano-sized metastable η′ (MgZn) type phases. Then the alloy in both states was subjected to HPT at room temperature (RT) up to effective strain of $e \sim 7$ under applied pressure of 5 MPa.

It was found that the HPT to maximum strains resulted in non-equilibrium nanostructure in both initial states (Fig. 1a, b). In the UA alloy, it was a mixed subgrain/cell one, composed by equiaxed (50 – 80 nm in diameter) and elongated (300 nm in length) crystallites, predominantly separated by LABs. However, in the Q state the crystallites were mostly equiaxed with more distinct boundaries. Moreover, the hardness increase in the Q alloy was more intense in the earlier SPD stages, followed by saturation at high strains, while in UA state, the hardness grew gradually, approaching the same saturation value (Fig. 1c). Thus, it was concluded, that the kinetics of grain refinement, as the morphology and parameters of the SPD-induced structures were surely conditioned by the effect of the heterogeneity of the initial structure: the higher were the densities of nanosized precipitates in the alloy matrix, the less-developed nanostructure was formed under SPD. Inhibition of dynamic recovery and homogenization of dislocation slip were determined as the main cause of such an alloy behavior [28].

2.2. Effect of grain size, TM contents and overaging

In [14, 29 – 31], hot-extruded rods of middle-strength 1420 alloy of standard composition (Al-5.5Mg-2.1Li-0.12Zr), having partially ($d = 7$ μm, $V_{rec} = 35\%$) and completely ($d = 5$ μm, $V_{rec} = 95\%$) recrystallized structures (coarse- and fine-grained (CG and FG rods, consequently), and also CG homogenized ingot, ($d \sim 47$ μm) with less amount of Zr (0.09%), were also processed by HPT. Prior to SPD, the samples were solution treated, quenched in water and part of them were further overaged (OA) at various temperatures and times. Unlike the Q alloys with the unimodal size distribution of precipitates of Zr aluminides with a mean diameter about 20 nm, the OA states had bimodal distribution of secondary phases, owing to additions of δ-(Al-Li) and S- (Al_2LiMg) phases of larger sizes (in the range of 150 – 600 nm) and fewer densities.

It was found that the nanostructures obtained were non-equilibrium fragmented (of grain/subgrain type) ones with a quite similar morphology (Fig. 2a, c). Basing on these data, no effects of the initial structure and its heterogeneity on severely deformed structures were detected. However, the effects have been observed in post-SPD annealed alloys, that is after transformation of deformation structures into equilibrium nano-grain ones owing to static recovery and recrystallization (Fig. 2b, d). As a result, in OA states, the coarser grains were formed regardless the dispersion of the strengthening phases prior SPD. Besides, an insignificant influence of the initial grain size on the final one was also observed in the Q alloys. Such a behavior was conditioned by the dynamic and static decomposition of the aluminum solid solution, suppressing the dislocation rearrangement and grain/subrgrain boundary movement by forming GP-zones and metastable phases and complicating thereby coalescence and growth of subgrains and grains. On the opposite, precipitation and coagulation of strengthening phases before SPD had a minor effect on grain boundary mobility, allowing both these processes. The largest grain size found in the preliminarily heterogenized ingot (Fig. 2d) was reasoned by the smaller density of TM aluminides owing to the smaller Zr content.

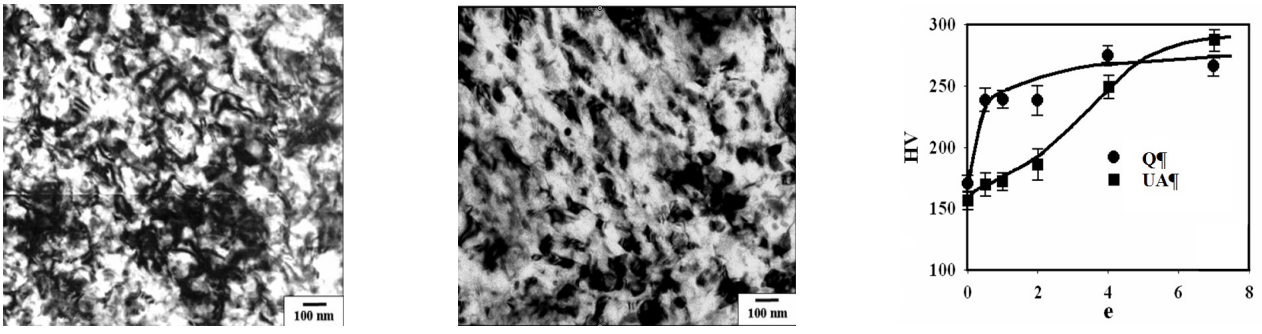

a b c

Fig. 1. Typical TEM structures of the preliminarily as-quenched (Q) (a) and further underaged (UA) (b) 7475Zr alloy after HPT (RT, $e = 7$, $P = 5$ GPa) and corresponding hardness changes with true strain (c) [28].

2.3. Effect of size, densities and nature of precipitates

The most detailed analysis of the influence of precipitates of different origin was performed in [32 – 34] for the high-strength 1965 (Al-8.1Zn-2.2Mg-2.3Cu-0.27Sc-0.10Zr-0.10 Mn) alloy. The homogenized ingots were processed by HPT (10 turns, 6 GPa, RT) in the Q, UA, PA (peak-aged) and OA (OA1 and OA2) conditions.

Unlike the Q state with coherent $Al_3(Zr,Sc)$ precipitates of about 20 nm in diameter, with density of 3×10^3 μm^{-3} and unimodal size distribution, the aged ones contained also the main strengthening η-type phases from 5 to 60 nm in equivalent diameter and with densities in the range of $5\times10^4 - 2\times10^3$ μm^{-3}, consequently (Fig. 3). In UA and PA conditions the precipitate distribution was bimodal, in OA1 — unimodal and in OA2 — also bimodal. The main distinction of OA1 from UA and PA states was in η-type phases coarsened to sizes of TM aluminides. Besides, the origin of bimodality in OA2, UA and PA states was different, as the second mode in the first one was formed by stable coagulated η-phases with corresponding decrease in their densities and volume fractions, and in the latter ones — by TM aluminides.

As in previously discussed studies, TEM analysis after SPD has revealed well-developed nanostructure of the matrix in the Q alloy with the mean fragment size of ~80 nm (Fig. 4a, b). However, the preliminary under- and peak-aging at 170°C, 10 hrs resulted in the highly work-hardened solid

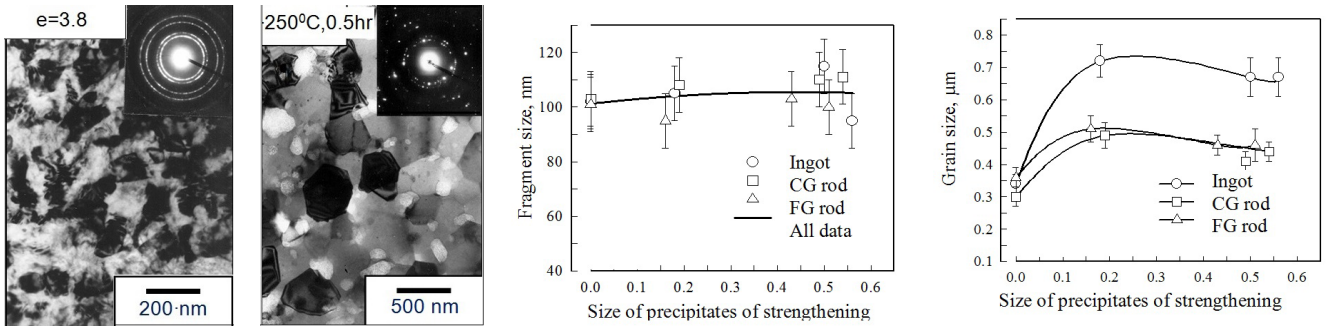

Fig. 2. Typical TEM structures of pre-quenched 1420-type alloys after HPT (RT, $P=6$ GPa) (a) and further annealing (b), and dependencies of their fragment (c) and grain (d) sizes on average size of δ and S strengthening phases prior HPT [14].

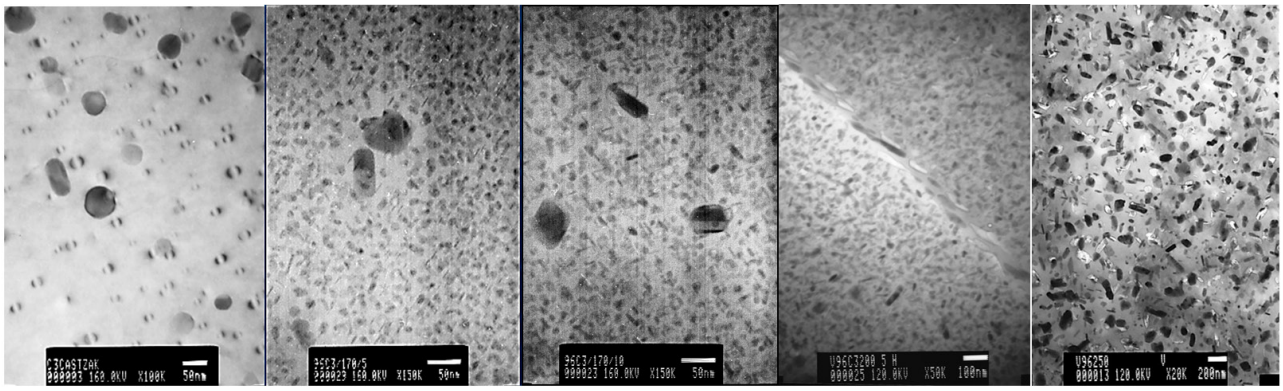

Fig. 3. Precipitates in the 1965 alloy after quenching (a), further 5 and 10 hrs aging at 170 (b and c) and overaging at 200 (d) and 250°C (e). $Al_3(Zr,Sc)$ phases are visible in (a), (b-e) illustrates η-type phases of different composition, shape, size and density.

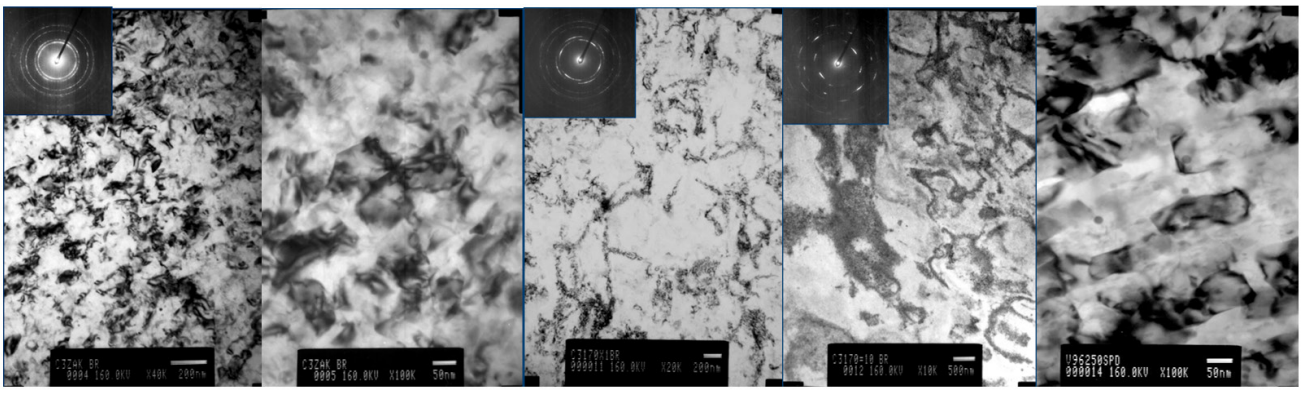

Fig. 4. TEM structures of Q (a and b), UA and PA (170°C, 1 and 10 hrs) (c and d), and OA2 (e) (250°C, 5 hrs) 1965 alloy after HPT.

solution with high densities of homogeneously distributed dislocations, being free of any features of recrystallization or polygonization (Fig. 4c, d). That means complete suppression of nanostructuring of the matrix. It was reasoned by an order of magnitude increase in density of nanosized precipitates under aging, leading to an increased homogeneity of macro- and microplastic deformation. Meanwhile, nanostructure, differed from that in the Q alloy by non-equiaxed shape of crystallites and their somewhat larger size, has been found in both OA samples (Fig. 4). This testifies that the matrix is able to dynamic recrystallization when the densities of the main strengthening phases are of the same order or less, than of secondary TM aluminides in conventionally treated ingots. It should also be noted that the nanostructure in the OA alloys was quite similar to that processed in the UA 7475 alloy [28] and can also be associated with the development of a spatial net of microshear bands, intersecting the elongated cellular substructures with high densities of lattice dislocations.

Another important finding was incomplete dissolution of secondary phases under SPD to high strains, which was frequently observed in Al alloys after HPT [4,8]. Moreover, both types of precipitates were TEM detectable in all structures processed. These data give us two important assumptions: a) TM aluminides still exist after SPD and remain coherent in unrecrystallized matrix in pre-aged conditions, testifying no changes in their orientation within the surrounding aluminum lattice; and b) the contribution of dispersion strengthening in the alloy strength has no sense changes under HPT.

Despite the low temperature deformation to actual high strains, heterogeneity of the initial structure significantly affected the alloy hardness and tensile strength after SPD (Fig. 5a, Table 1). Being in a good agreement with the alloy structure transformations, the Q alloy demonstrated the strength higher than in other states. Its initial strength was conditioned by three main factors: a) strength of pure aluminum (Peierls-Nabarro force); b) aluminum solid solution hardening due to the supersaturization by main alloying elements (Zn, Mg, Cu); and c) dispersion strengthening of the matrix by TM aluminides. These three contributions gave the alloy hardness of about 110 HV (Fig. 5a). Further peak-aging owing to η-phase dispersion hardening increased it on about 80 – 90 HV. Under HPT the pre-quenched alloy possessed work- and grain boundary strengthening with a total amount of about 150 – 160 HV, giving the hardness up to 270 HV. Such a level is mainly conditioned by an increase in dislocation density and also by grain and subgrain refinement, being the maximum in the Q state. At that time, preliminary minimum solution and η-phase dispersion strengthened OA states with hardness of about 80 HV possessed nearly similar strengthening under HPT and resulted in hardness of about 200 – 220 HV. Thus, these data give us a conclusion, that the pure effect of the alloy nanostructuring under HPT, accompanied by increase in dislocation density and formation of nanoscale network of non-equilibrium subgrain/grain boundaries, is limited by the value of about 150 HV. Taking into account the hardness of UA and PA alloys before and after HPT, the contributions of both work- and grain boundary strengthening could be estimated each, as about 70 – 80 HV. It is a bit less than the dispersion strengthening under conventional aging.

The data in Table 1 also have proved the strong dependence of the tensile strength of the SPD-ed alloy on initial structure heterogeneity. The maximum strengthening was found in Q alloy, causing by the formation of the most-developed nanostructure. However, the alloy ductility is critically low with elongations to failure not exceeding 2.5%. Meanwhile, the pre-aged alloy showed about 25% reduced yield strength along with significantly enhanced ductility. Thus, suppression of the matrix nanostructuring owing to implementation of a preliminary aging into nanoTMT, resulted in its less structural hardening. Therewith, this hardening was too close to the level found in commercial T1-tempered hot-pressed rod (Table 1), that realized the effect of substructure hardening and dispersion strengthening.

Table 1. The 1965 alloy mechanical properties.

Condition	Hardness, HV	YS, MPa	UTS, MPa	El, %
T1 (rod) (min)	210	690	720	4
Q + HPT	270 ± 10	990 ± 40	1030 ± 35	2.1 ± 0.5
UA + HPT	235 ± 15	745 ± 25	800 ± 25	7.6 ± 2.1
PA + HPT	225 ± 15	750 ± 40	795 ± 40	7.4 ± 2.0
OA1 + HPT	225 ± 10	820 ± 20	880 ± 30	1.5 ± 1.0

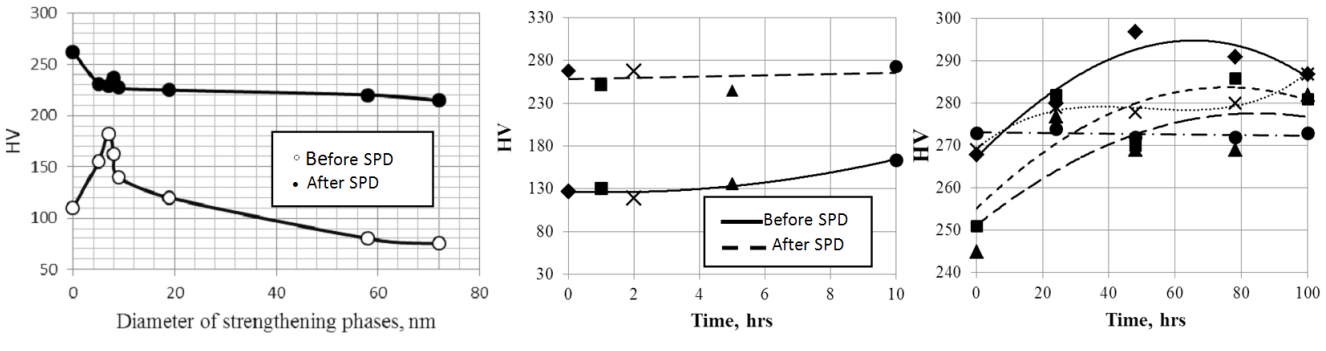

a b c

Fig. 5. Evolution of the 1965 (a) [34] and D16 (b and c) [37] alloys hardness vs (a) — initial size of η phase precipitates, (b) — time of aging at 190°C and (c) — time of further re-aging at 100°C. Symbols in (c) correspond to duration of preliminary aging in (b).

2.4. Effect of aging and re-aging.

In [35,36] the effect of disperse strengthening phases, whose parameters were varied by changing the duration of artificial aging under the standard preliminary strengthening heat treatment, on nanostructuring of the 2xxx alloy was investigated. In addition, the response of the alloy hardening at SPD and post-SPD re-aging was measured. With this aim the hot-pressed aluminum alloy D16 of a standard composition (Al-4Cu-1Mg-0.4Mn) was subjected to room temperature HPT with 10 turns at $P = 6$ GPa. Preliminarily the alloy was solution treated at 505°C and water quenched, then artificially aged at 190°C (at a temperature of standard T1 route) in the range from 1 to 10 hrs (10 hrs annealing corresponds to PA (T1) condition). As a result, the Q state was characterized by the supersaturated by Cu and Mg aluminum matrix with fairly uniform distributed particles of T-phase ($Al_2Mn_3Cu_2$) having average length and thickness of 330 and 70 nm, respectively, and density of 3×10^2 μm^{-3}. In the pre-aged alloy, owing to decomposition of aluminum solid solution, in addition to these phases, zones and metastable nanosized lamellar precipitates of the strengthening S-phase (Al_2MgCu) were formed. Their sizes increased and densities decreased with aging time and reached 205×8 nm and 4×10^3 μm^{-3}, respectively, after 10 hrs aging.

As in previous studies, the most uniform and developed nanostructure of a matrix with an average fragment size about 70 – 80 nm and high dislocation density was formed in the Q alloy. Pre-aging led to some suppression of SPD nanostructuring and increasing the fraction of areas with high dislocation densities (dense dislocation walls). Judging by the data in Fig. 5b, these structural differences resulted in near equal hardness of all conditions processed, in spite of typical alloy aging response. Thus, after small aging times, no significant hardness changes were observed; and in PA alloy the dispersion strengthening prevailed over solid solution softening and provided a hardness gain till 40 – 45 HV. However, SPD led to considerable alloy strengthening with unique high hardness values irrespective the initial state (Fig. 5b). Their difference before and after HPT indicates that the alloy in Q and UA conditions possessed the maximum strengthening owing to SPD. With increase in the aging time to PA point, the alloy extra hardening decreased. These data also testified that the strengthening under HPT is controlled by the heterogeneity of the initial structure. Therewith, the SPD-ed alloy strength is conditioned by two factors — increase in density of defects of a crystal structure (generally dislocations and their arrays), and formation of a net of new grain boundaries. The contribution from the last has a maximum in the Q alloy and decreased with aging time.

Carrying out the re-aging of SPD-ed alloy at 100°C up to 100 hrs has demonstrated a good potential to its additional hardening. The hardness increase on 15 – 30 Hv was observed in all conditions investigated, except PA one (Fig. 5c), causing that its value was in a right dependence on the preliminary degree of supersaturization of the aluminum solid solution. The most intense hardening was found during the first 50 hrs of re-aging. And even after 100 hrs, the effect was visible for Q and UA states, testifying also the strong effect on the initial alloy condition under complex nanoTMT with two aging steps — before and after SPD. These data give us one more proof to absence of a sense dissolution of precipitates of both types under HPT up to 10 turns at room temperature, determining the alloy strength and hardness values.

3. Summary

The structure and phase evolutions under HPT, as well as under prior- and post-deformation heat treatment studied, influence the structure and mechanical behavior of middle- and high-strength age-hardenable alloys in accordance with the well-known structure/property relationships, observed at their conventional TMTs. For instance, cold straining, realized by any techniques, commonly resulted in the alloy strengthening, as due to HPT. However, despite the extremely high strains and degree of work-hardening reached in the studies presented, the initial alloy condition significantly affected their structure transformations and strengthening. Therewith, the levels of hardness and tensile strength in the pre-quenched and SPD processed, nanostructured alloys were abnormally high compare with conventional products. Meanwhile, the SPD-ed alloys in the pre-annealed conditions demonstrate a considerably less strength and enhanced ductility, being in a good agreement with the type and homogeneity of the diffuse dislocation structure processed and the level of their initial hardness, determined by the degree of structure heterogeneity. Suppression of the nanostructuring because of preliminary artificial aging and formation of uni- or bimodal size distributions of nanoprecipitates with total densities not less than 10^4 μm^{-3}, could give the minimum structural hardening under HPT. Thus, these alloys, especially in the initially PA state, could demonstrate not only complete absence of nanostructuring of the matrix, but also low difference in strength before and after HPT, resulting in low efficiency of their nanoTMT.

The preliminary overaging, accompanied by increasing the size of precipitates and decreasing their density with annealing temperature and time, gives somewhat reduced hardness values after SPD. It has been conditioned by two facts: a) some loss in dispersion hardening of the initial state, owing to phase coarsening, resulted in the same effect in the processed alloy; and b) nanostructural strengthening of the alloy matrix was somewhat less than in the pre-quenched one due to formation of less-developed grain boundary net with a larger spatial size (spacing). However, in distinction with under- and peak-aged conditions, the difference in hardness between initial and SPD-ed OA states is much higher and near equal to found in Q conditions, testifying the potential of hardening of HPT processing.

Meanwhile, the SPD-ed alloys can possess extra hardening being realized at their post-deformation aging. For that the alloys have to deform in the preliminarily quenched or underaged conditions.

Thus, the nanoTMT, involving preliminary quenching, cold HPT, and post-SPD low-temperature aging is the most effective route to impart superstrength to age-hardenable aluminum alloys conditioned by the synergy effect of well-developed nanostructure, high densities of dislocations and high densities of precipitates.

Acknowledgments. The authors are thankful to the Russian Science Foundation for funding this research under grant № 16-19-10152.

References

1. N.P. Lyakishev. Tech. Light Alloys. 3, 40 (2006). (in Russian) [Н.П. Лякишев. ТЛС 3, 40 (2006)].
2. R.A. Andrievsky, A.M. Glezer. Physics-Uspekhi. 52, 315 (2009).
3. V.I. Elagin. Tech. Light Alloys. 2, 6 (2008). (in Russian) [В.И. Елагин. ТЛС 2, 6 (2008)].
4. R.Z. Valiev, A.V. Korznikov, R.R. Mulyukov, Mat. Sci. Eng. A 168, 141 (1993).
5. V.M. Segal. Mater. Sci. Eng. A 197, 157 (1995).
6. F.J. Humphreys, P.B. Prangnell, J.R. Bowen, A. Gholinia, C. Harris. Phil. Trans. R. Soc. Lond. A357, 1663 (1999).
7. M.V. Markushev. Letters on Materials. 1(1), 36 – 42 (2011) (in Russian) [М.В. Маркушев. Письма о материалах 1(1), 36 – 42 (2011)]. DOI: 10.22226/2410-3535-2011-1-36-42
8. R.Z. Valiev, Y. Estrin, Z. Horita, T.G. Langdon, M.J. Zehetbauer, Y.T. Zhu. JOM. 68, 1216 (2016).
9. R.Z. Valiev, I.V. Aleksandrov. Bulk Nanostructured Metallic Materials: Processing, Structure, and Properties — Moscow: Akademkniga. 2007 (in Russian) [Р.З. Валиев, И.В. Александров. Объемные наноструктурные металлические материалы: получение, структура и свойства. М.: Академкнига, 2007].
10. R.Z. Valiev, Y. Estrin, Z. Horita, T.G. Langdon, M.J. Zehetbauer, Y.T. Zhu. Mater. Res. Lett., 4, 1 (2016).
11. K. Kosuge, K. Takeuti, Bull. Jap. Inst. Metals. 21, 104 (1982).
12. E. Nes and J.A. Wert, Scr. Met. 18, 1433 (1984).
13. J.A. Wert, N.E. Paton, C.H. Hamilton, M.W. Mahoney, Metall. Trans. A. 12A, 1267 (1981).
14. M.V. Markushev, Phys. Met. Metallogr. 8, 161 (2009).
15. F.J. Humphreys, Acta Met. 25, 1323 (1977).
16. F.J. Humphreys, M. Hatherly. Recrystallization and Related Annealing Phenomena, 2nd ed. — Amsterdam: Elsevier. 2004. 658 p.
17. M.V. Markushev. Phys. Met. Metallogr. 7, 43 (2009).
18. O. Sitdikov, E. Avtokratova, R. Babicheva. Phys. Met. Metallogr. 2, 153 (2010).
19. C.Y. Barlow, N. Hansen, Y.L. Liu. Acta Mat. 50, 171 (2002).
20. M.V. Markushev, M.Yu. Murashkin, C.C. Bampton, D.A. Hardwick. Mater, Sci. Eng. A. 234 – 236, 927 (1997).
21. M.V. Markushev, M.Yu. Murashkin. Phys. Met. Metallogr. 90, 506 (2000).
22. M.V. Markushev, M.Yu. Murashkin. Phys. Met. Metallogr. 98, 221 (2004).
23. M.V. Markushev, M.Yu. Murashkin. Mater. Sci. Eng. A, 367, 234 (2004).
24. M. Markushev, A Vinogradov. Room Temperature Mechanical Properties of Submicrocrystalline Commercial Aluminum Alloys Processed by Severe Plastic Deformation. In Severe Plastic Deformation: Towards Bulk Production of Nanostructured Materials, (ed) Burnhanettin Altan, Nova Science Publishers, USA, 2006, pp. 233 – 247.
25. M.V. Markushev, Probl. Mat. Sci., 52, 217 (2007).
26. E. Avtokratova, O. Sitdikov, M. Markushev, R. Mulyukov. Mat. Sci. Eng. A. 538, 386 (2012).
27. R.R. Mulyukov, R.M. Imayev, A.A. Nazarov, etc. Superplasticity of ultrafine-grain alloys: experiment, theory, technologies. Moscow: Nauka, 2014, 284 p. (in Russian) [Р.Р. Мулюков, Р.М. Имаев, А.А. Назаров и др. Сверхпластичность ультрамелкозернистых сплавов: эксперимент, теория, технологии. М.: Наука, 2014, 284 с.
28. O. Sitdikov, S. Krymskiy, M. Markushev, E. Avtokratova, T. Sakai. Rev. Adv. Mater. Sci. 31, 62 (2012).
29. M.Kh. Rabinovich, M.V. Markushev, M. Yu Murashkin. Met. Sci. Heat Treat. 39, 172 (1997).
30. M.Kh. Rabinovich, M.V. Markushev, M.Yu. Murashkin. Mater. Sci.Forum 243 – 245, 591 (1997).
31. M.V. Markushev, M.Yu. Murashkin, M.Kh. Rabinovich. Proc. TMS Meeting on Superplasticity and Superplastic Forming. The Minerals, Metals and Materials Society, Warrendale, Pa. 1998, pp. 3 – 13.
32. S. Krymskiy, O. Sitdikov and M. Markushev. AIP Conf. Proc. 1785, 040030 (2016); DOI: 10.1063/1.4967087.
33. M.V. Markushev, Yu.L. Burdastykh, S.V. Krymskiy, O.Sh. Sitdikov. Letters on Materials. 7(2), 101 – 104 (2017). DOI: 10.22226/2410-3535-2017-2-101-104
34. M.V. Markushev, E.V. Avtokratova, S.V. Krymskiy, O.Sh. Sitdikov. J. Alloys Comp. (2018) (in press).
35. M.V. Markushev, E.V. Avtokratova, R.R. Ilyuasov, S.V. Krymskiy, O.Sh. Sitdikov. Russian Metallurgy (2018) (in press).
36. M. Markushev, S. Krymskiy, E. Avtokratova, R. Ilyasov, O. Sitdikov, AIP Conf. Proc. (2017) (in press).
37. M.V. Markushev, E.V. Avtokratova, R.R. Ilyasov, S.V. Krymskiy, O.Sh. Sitdikov. Phys. Mech. Mater. (2017) (in press). (in Russian) [М.В. Маркушев, Е.В. Автократова, Р.Р. Ильясов, С.В. Крымский, О.Ш. Ситдиков. Физика и механика материалов 2017 (в печати).]